



海洋地质与第四纪地质

MARINE GEOLOGY & QUATERNARY GEOLOGY

柴达木盆地西北部中新世矿物学特征及其古气候意义

秦秀玲, 常 宏, 关 冲

Mineralogical characteristics and paleoclimatic significance of the Miocene deposit in the northwestern Qaidam Basin

QIN Xiuling, CHANG Hong, and GUAN Chong

在线阅读 View online: <https://doi.org/10.16562/j.cnki.0256-1492.2024010901>

您可能感兴趣的其他文章

Articles you may be interested in

晚中新世柴达木盆地低偏心率时期倾角驱动的干湿变化

Obliquity-driven moisture changes in Qaidam Basin in Late Miocene during low eccentricity period

海洋地质与第四纪地质. 2022, 42(6): 193–199

南薇西含油气盆地地层层序及生储盖组合特征

Characteristics of stratigraphic sequence and the source–reservoir–cap assemblages in the Nanweixi petroliferous basin

海洋地质与第四纪地质. 2021, 41(6): 163–173

珠江口内伶仃洋晚第四纪黏土矿物组成特征及对源区气候变化的指示

Late Quaternary clay minerals in the inner Lingdingyang of the Pearl River Estuary, southern China: Implications for paleoclimate changes at the provenance

海洋地质与第四纪地质. 2021, 41(5): 202–209

印度尼西亚库泰盆地下中新统混积序列特征研究

Characteristics of Lower Miocene mixed deposits in Kutai Basin, Indonesia

海洋地质与第四纪地质. 2022, 42(2): 158–166

铜川地区早中全新世黄土沉积特征及其古气候意义

Sedimentary characteristics of the Early and Middle Holocene loess in Tongchuan area and their implications for paleoclimate

海洋地质与第四纪地质. 2020, 40(1): 160–166

北康-曾母盆地中新世以来层序地层样式特征探讨

The characteristics of the system domain and the stratigraphic framework of the Beikang–Zengmu Basin since the Middle Miocene

海洋地质与第四纪地质. 2022, 42(3): 111–122



关注微信公众号，获得更多资讯信息

秦秀玲, 常宏, 关冲. 柴达木盆地西北部中新世矿物学特征及其古气候意义 [J]. 海洋地质与第四纪地质, 2025, 45(2): 177-188.
QIN Xiuling, CHANG Hong, GUAN Chong. Mineralogical characteristics and paleoclimatic significance of the Miocene deposit in the northwestern Qaidam Basin[J]. Marine Geology & Quaternary Geology, 2025, 45(2): 177-188.

柴达木盆地西北部中新世矿物学特征及其古气候意义

秦秀玲^{1,2}, 常宏¹, 关冲^{1,3}

1. 中国科学院地球环境研究所黄土与第四纪地质国家重点实验室, 西安 710061

2. 中国科学院大学, 北京 100049

3. 中国地质调查局西安地质调查中心, 西安 710119

摘要: 中中新世气候适宜期是新生代气候变冷背景下的一次短期气候变暖事件。研究此阶段沉积物记录的环境特征对预测未来全球变暖背景下气候变化趋势具有指导意义。亚洲内陆极端干旱区中中新世气候适宜期记录较少, 而且该时段气候变化的受控因素仍未明确。本研究通过柴达木盆地北部花土沟剖面中新统矿物分析, 明确了中新世全球气候变化重要事件在柴达木盆地环境变化过程中的响应, 重点探讨黏土矿物干湿指标反演的柴达木盆地该时段古气候演化历史以及驱动机制。结果显示, 柴达木盆地早—中中新世期间 (17.2~15.2 Ma) 气候最为温暖湿润, 主要受全球中新世暖期气候的影响。15.2~12.4 Ma 柴达木盆地气候波动变干, 盆地受区域构造与中中新世降温事件的共同影响。12.4~11.3 Ma 柴达木盆地持续变干, 主要受全球气候的影响。全球气候及区域构造运动共同影响柴达木盆地早—中中新世气候。

关键词: 矿物组合; 构造运动; 古气候; 中新世; 柴达木盆地

中图分类号:P532 文献标识码:A DOI: [10.16562/j.cnki.0256-1492.2024010901](https://doi.org/10.16562/j.cnki.0256-1492.2024010901)

Mineralogical characteristics and paleoclimatic significance of the Miocene deposit in the northwestern Qaidam Basin

QIN Xiuling^{1,2}, CHANG Hong¹, GUAN Chong^{1,3}

1. State Key Laboratory of Loess and Quaternary Geology, Institute of Earth Environment, Chinese Academy of Sciences, Xi'an 710061, China

2. University of Chinese Academy of Sciences, Beijing 100049, China

3. Xi'an Center of Geological Survey, China Geological Survey, Xi'an 710119, China

Abstract: The Middle Miocene Climatic Optimum (MMCO) is a short-term climate warming event interrupting the background of Cenozoic climate cooling. Study on the environmental characteristics based on sediments is important for predicting the trend of climate change with the global warming in the future. There are few records of the MMCO in the extreme arid interior of Asia, and the controlling factors of paleoclimate changes are still unclear. The mineral assemblages of the Miocene sediments from the Huatugou section in the northern Qaidam Basin were analyzed, the regional response to the global climate event and the environmental change in the Qaidam Basin during early-middle Miocene were revealed, and the paleoclimate evolution including the shifting and driving mechanisms of relative moisture index of clay minerals were focused. Results show that during the early-middle Miocene in Qaidam Basin, the climate during 17.2~15.2 Ma was the warmest and wettest, which should belong to the MMCO and mainly affected by the global climate. The climate in the basin began to fluctuate and became dried during 15.2~12.4 Ma. The basin was affected by the regional geological structure and the Middle Miocene cooling event. From 12.4 to 11.3 Ma, Qaidam Basin continued to dry out, mainly under the influence of global climate again. We pointed out that the global climate change trend and regional tectonic movement influenced the early and middle Miocene climate in Qaidam Basin.

Key words: mineral assemblage; tectonic movement; paleoclimate; Miocene; Qaidam Basin

资助项目:国家自然科学基金项目“塔里木盆地钻孔岩芯记录的上新世气候变化特征及其影响因素”(4237221);第二次青藏高原综合科学考察项目“高原风化剥蚀历史及气候环境效应”(2019QZKK0707);黄土与第四纪地质国家重点实验室开放基金资助项目“柴达木盆地中中新世大暖期沉积序列的黏土矿物学研究”(SKLLQG2121)

作者简介:秦秀玲(1990—),女,硕士研究生,主要从事第四纪地质与全球变化研究, E-mail: qinxiuling@ieecas.cn

通讯作者:常宏(1970—),男,研究员,主要从事第四纪地质与全球变化研究, E-mail: changh@loess.llqg.ac.cn

收稿日期:2024-01-09; 改回日期:2024-04-03. 文凤英编辑

中新世适宜期(17~15 Ma, MMCO)是距今较近且未受人类活动影响的相对气候暖期, MMCO时期全球大气二氧化碳含量与现今基本相似^[1-2], 当时年均温比现在高3~6°C^[3-6]。之后的中新世转型期(MMCT), 全球平均温度下降超过了5°C^[3-7], 气温从相对温暖湿润的适宜期进入寒冷干燥的转型期, 研究此时期气候环境特征可为预测未来全球变暖背景下气候变化趋势提供可参考的自然模型。

长期以来, 青藏高原生长受到人们的广泛关注, 高原隆升不仅使大气环流发生变化, 影响亚洲内陆气候^[8-10], 而且还会加强硅酸盐化学风化, 进而使大气二氧化碳含量降低, 促使全球气温降低^[11-12]。青藏高原生长-气候变化之间的耦合关系是地球科学关注的焦点和热点问题, 也是地学界极富挑战性的科学问题。研究者认为亚洲内陆新生代气候变化的主控因素可能为全球变冷、主要山脉和青藏高原隆升以及特提斯海退等^[13-16]。中新世青藏高原强烈的构造运动改变了该地区的降水模式^[13, 17-19], 从而使亚洲内陆中新世的气候特征更为复杂。这增加了对该时期区域气候变化驱动因素研究的难度。对亚洲内陆中新世沉积序列的研究可以更好地帮助我们理解该区域中新世气候变化可能的驱动机制。到目前为止, 对亚洲内陆MMCO和MMCT事件的研究基本上基于亚洲季风区或半干旱区域^[20-21], 亚洲内陆极端干旱区中新世沉积记录相对较少。柴达木盆地主要受西风带的控制, 气候极端干旱。柴达木盆地是青藏高原构造活跃区、西北内陆干旱区以及高原高寒区的交汇地带, 盆地内巨厚且连续的河湖相沉积地层^[18-19]比较完整地记录了新生代盆地变形、气候变化和化学风化等信息^[17, 19, 22-40], 是解决上述问题的理想区域载体。

黏土矿物在沉积物中较为常见, 根据沉积序列中黏土矿物种类与含量变化提取的古气候信息, 与其他方法获得的气候指标能够完美地对比^[41-42]。黏土矿物研究已在山体构造和气候演化中得到广泛应用^[43-44]。本文通过柴达木盆地新近系黏土矿物干湿代用指标、重矿物组成的研究, 建立柴达木盆地早—中新世古环境演化序列, 结合全球与区域资料, 探讨其可能的驱动因素。

1 地质概况

1.1 柴达木盆地概况

柴达木盆地位于青藏高原东北部, 面积约

12万km², 作为青藏高原与周边较低区域的过渡位置凸显了其在青藏高原演化研究中的重要意义。柴达木盆地周边被高大的山脉围绕, 西北为阿尔金山, 东北为祁连山, 南面则为东昆仑山(图1), 这些山体的雨影效应使盆地多年平均降水量小于100 mm, 盆地内部主要以盐湖或沙漠地貌为主。盆地平均海拔3000 m, 与周边山脉之间均以断裂构造为界—西北、东北、南面分别以阿尔金左行走滑断裂(ATF)、柴北缘逆冲断裂(NQTS)及昆仑逆冲断裂(KLF)为界^[40, 45-47]。由于新生代盆地主要受到印度板块和欧亚板块挤压远程效应的影响^[48], 昆仑山和祁连山之间生成大量的北西向的断层。位于西北部的阿尔金走滑断裂的同期活动, 使柴北缘出现压扭性的反S形断裂系统^[49]。始新世以来柴达木盆地沉积中心沿着盆地轴线自西北向东南偏移^[47, 50-51]。新生代柴达木盆地的物源分析显示柴达木盆地碎屑主要来自周围山体, 尤其是阿尔金山^[52]。柴达木盆地新生界地层是研究青藏高原构造运动及区域古气候演化的良好载体。

柴达木盆地新生界主要为河湖相沉积物, 根据岩性特征、化石组合以及接触关系, 盆地沉积物地层序列从新到老可分为7个地层单元, 依次为七个泉组、狮子沟组、上油砂山组、下油砂山组、上干柴沟组、下干柴沟组和路乐河组。

1.2 花土沟地质概况

花土沟剖面位于柴达木盆地的西北部(图2), 油砂山背斜的西南翼, 介于38°22.0'~38°25.6'N、90°52.9'~90°53.8'E之间, 周边山体风化剥蚀产物通过河流、风等外力地质作用搬运汇入该区并沉积下来。花土沟剖面记录了柴达木盆地渐新世—中新世山体的构造生长过程以及周边的环境变化^[40, 45, 52, 54], 是研究柴达木盆地中新世构造生长和环境变化的理想场所。

花土沟剖面新生界总厚度大于4386 m, 从下到上依次是上干柴沟组(0~895 m)、下油砂山组(895~3698 m)以及上油砂山组(3698~4216 m)^[40, 45]。

花土沟剖面上干柴沟组是由分选性较好的灰色细砂和粉砂岩组成, 里面含有泥晶质碳酸盐并夹杂着分选性较差的碎屑砾岩和石膏层, 该组的448.8 m和762 m分别发现了两具鱼类化石, 该层基本属于渐新世河流相或者湖泊边缘相沉积环境。

剖面上干柴沟组古地磁解释存在不单一性^[40]。本次研究剖面选1363.2~4196.2 m段, 其古地磁年

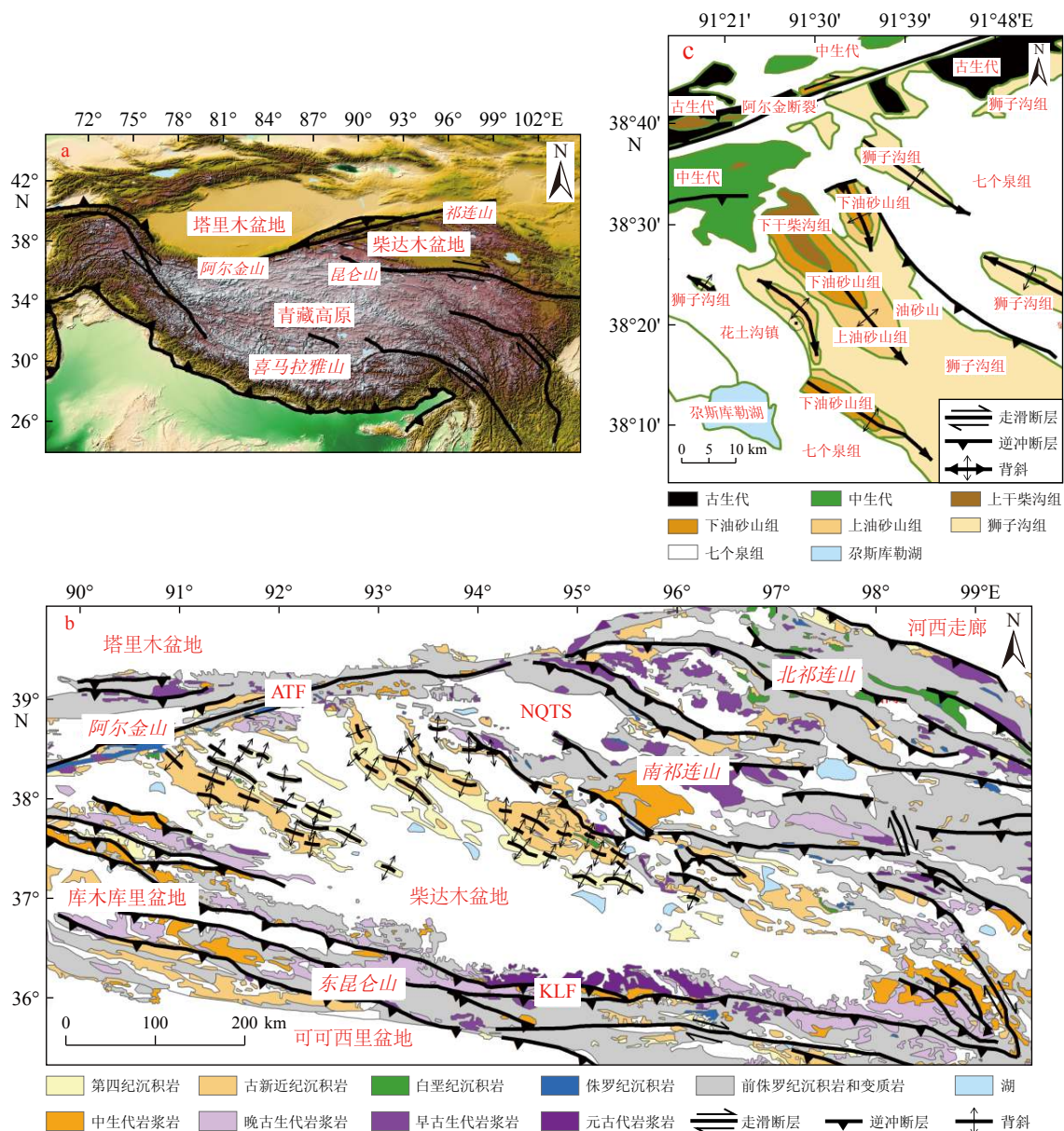


图 1 研究区及周边地质形貌概况图

改自文献 [40, 53]。a: 柴达木盆地地理位置, b: 柴达木盆地地质概况图, c: 油砂山地质概图。

Fig.1 Geomorphology of the study area and surrounding areas

Modified from reference [40, 53]. a: Geographical location of Qaidam Basin, b: tectonic setting of Qaidam Basin, c: geological background in the Youshishan region.

代为 20.0~11.3 Ma^[40], 为早中新世沉积。岩性描述如下(图 3):

下油砂山组, 1363.2~3 698 m(20.0~12.4 Ma), 其中 1363.2~2 712 m(20.0~14.1 Ma)段主要由灰绿色—棕红色泥岩、粉砂岩及细砂岩组成, 含少量砾岩, 发现鱼类化石。2 712~3 698 m(14.1~12.4 Ma)段泥岩—粉砂岩减少, 砾岩明显增多, 碎屑粒径向上逐渐变粗。下油砂山组是向上逐渐变浅的湖泊边缘相沉积^[40, 52]。

上油砂山组, 3 698~4 196.2 m(12.4~11.3 Ma), 主要为砾岩, 含有少量的层状—透镜状粉砂岩和砂岩, 分选差, 沉积物粒度向上变粗。该组属于河流相沉积^[40]。

2 研究方法

以 20~30 m(时间分辨率小于 0.1 Ma)间隔取样, 共采集了 106 个样品。每个样品取 1.5 g 敲碎

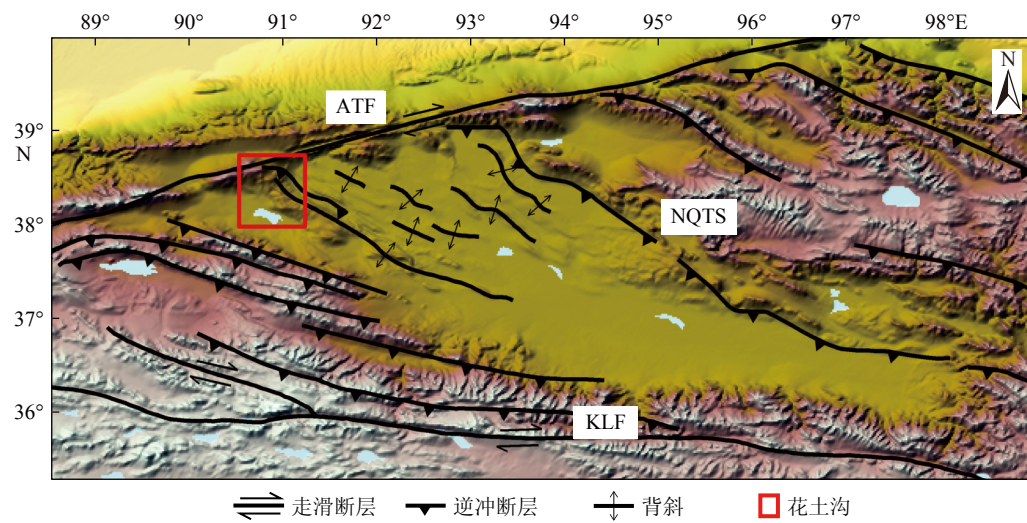
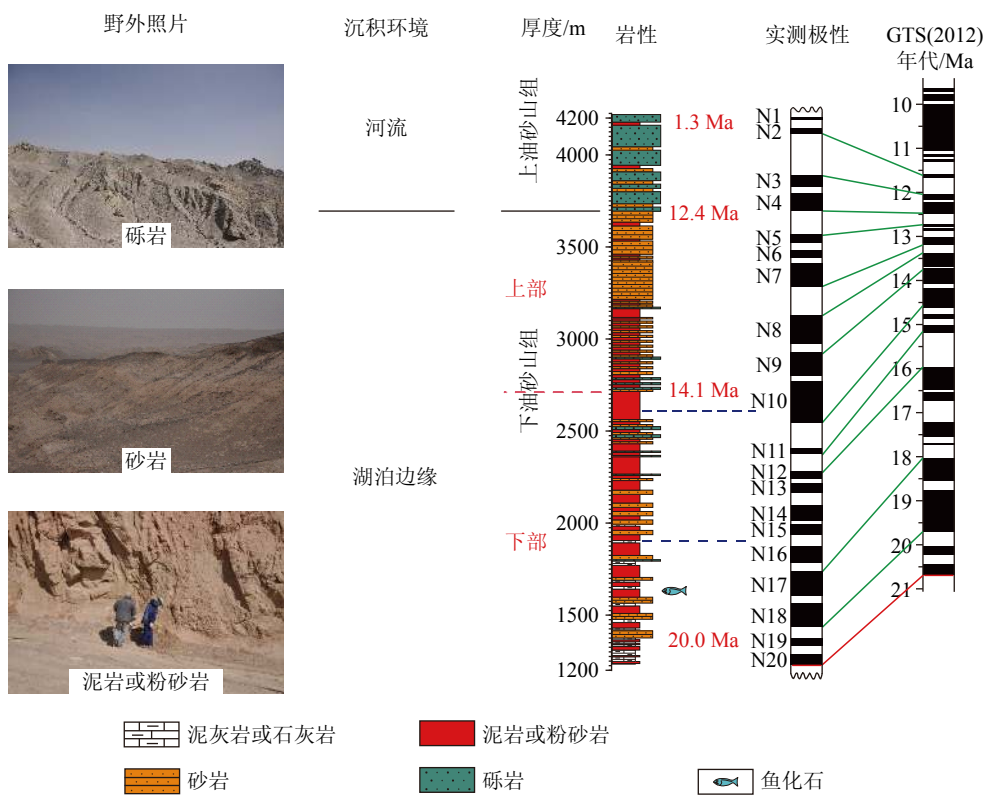


Fig.2 Morphotectonic map of the Qaidam Basin and locations of the Huatugou section

Modified from reference [40].



(极细砂粒径大小)。将样品与环氧树脂组合液(质量比为25:7的环氧树脂和凝固剂)混合,混合时用超声仪超声使样品与混合液分散均匀,将分布均匀的混合液用抽真空仪抽真空20 min,排除混入的气泡,将抽完真空的混合液二次放入超声仪中超声,

使气泡完全排除,同时混合液基本定型没有流动性后,放入烘箱中凝固8 h取出,进行水(粗抛)抛光和金刚砂(细抛)抛光处理即可得到矿物测试样本。利用德国蔡司配合能谱仪(EDS)的EVO 18多用途扫描电镜分析系统进行测试分析。

矿物自动定量分析系统(Advanced/Automatic Mineral Identification and Characterization System, AMICS)的硬件设备是由扫描电镜和X射线能谱仪组成, 测试前根据样品特征和测试要求设置好测试参数, AMICS 就可直接操控电镜和能谱对样品进行自动测试。AMICS 将 SEM 获得的背散射图进行背景扣除、颗粒化以及矿物颗粒相分离等处理后, 结合 X 射线能谱仪的矿物元素测试结果而得到含矿物组成信息的矿物样品图。最后将矿物样品图与含有 2 000 多种矿物的标准数据库进行比对与计算, 获得矿物颗粒的种类、含量、元素组成、粒径大小、形貌特征等数据。

每个矿物样本矿物含量是基于扫描电镜和能谱(EDS)获得的大量(≥ 5000 个)矿物颗粒数据, 由 AMICS 矿物分析系统自动统计计算得出的结果。测试精度能达到 1‰, 测试结果相比于传统的显微镜矿物识别具有更高的精度和更准确的含量计算。实验测试在中科院地球环境研究所盆地分析实验室完成。

3 矿物学特征

3.1 黏土矿物

盆地沉积物黏土矿物能够详细地记录物源区岩石组成和流域内的化学风化程度^[55]。地表化学风化是各圈层相互作用的反映, 湖盆黏土矿物的形成受母岩类型、水文条件、区域生态特征及地区构造等因素影响。在地壳稳定的情况下, 黏土矿物的生成和转化主要受热量和水分等气候因素的影响^[41-42], 因此温暖湿润与干旱寒冷气候条件下生成的黏土矿物类型和含量存在差异。因此, 根据黏土矿物特征推测源区的物质组成和气候演化历史, 有助于重建区域古环境演化历史。

绿泥石主要由 Si^{4+} 、 Al^{3+} 、 Fe^{2+} 、 Mg^{2+} 阳离子组成, 在淋滤作用较弱条件下形成^[41, 44, 56]。因为绿泥石中含有的 Fe^{2+} 容易被氧化, 一般形成于抑制化学风化的冰川或干旱地区^[41-43, 57]。花土沟中新世沉积物主要为湖泊边缘-河流环境沉积^[40, 52]。干旱化增强时湖面降低或者转为河流相, 沉积环境很容易从相对还原的水下湖泊边缘相转为氧化性较高的河流相环境, 造成 Fe^{2+} 氧化而使绿泥石含量减少。伊利石中含有的主要阳离子是 Si^{4+} 、 K^+ 、 Al^{3+} , 通常由云母或长石等铝硅酸盐矿物在相对温暖或寒冷少雨的弱碱性条件下风化形成^[41-43]。当气候条件湿热

时, 伊利石会因发生更强的淋滤作用脱去 K^+ 而形成高岭石^[43]。因此, 伊利石主要分布在淋滤作用较弱的干冷环境中^[41-43]。降水充足时有利于绿泥石沉积, 降水减少的时期主要生成伊利石^[58]。伊利石/绿泥石可以代表温暖气候下区域干旱程度^[41], 进而有效地指示研究区气候的干湿变化特征。即: 伊利石/绿泥石值越高表示气候越干旱, 比值越低反映气候相对湿润。

AMICS 矿物测试系统得到的矿物数据, 挑选出粒径小于 4 μm 的单颗粒黏土矿物, 可以排除全岩矿物组分中碎屑岩矿物组分(代表源区母岩信息)和非硅酸盐矿物组分(主要为沉积环境产物)的影响, 最大程度地排除沉积分选对风化指标的影响^[59-60], 能较为准确地代表源区硅酸盐化学风化和古气候变化的信息。

本研究区的黏土矿物主要为伊利石和绿泥石, 蒙脱石和高岭石基本未发现, 说明当时研究区气候相对比较干旱, 环境可能呈弱碱性。花土沟剖面地处中纬干旱区, 黏土矿物为伊利石和绿泥石, 与现代气候环境相符。伊利石/绿泥石比值在 20.0~15.2 Ma 逐渐降低, 17.2~15.2 Ma 达到最低值, 15.2~11.3 Ma 波动升高(图 4)。伊利石/绿泥石比值曲线变化趋势在 20.0~14.4 Ma 和 12.4~11.3 Ma 时期变化趋势基本与全球 $\delta^{18}\text{O}$ 变化一致, 但在 14.4~12.4 Ma 时期与全球 $\delta^{18}\text{O}$ 变化趋势不同。

3.2 重矿物

重矿物具有耐磨损、易于保存等相对比较稳定的特点, 可以比较完整地保存母岩信息而常常被用于物源示踪^[61]。除了可以被用来指示同一时期母岩的沉积搬运距离和方向外, 重矿物的组合也可以反映不同历史时期的古气候演化以及构造历史^[62]。

花土沟中含有的重矿物为闪石、黑云母、绿帘石、辉石、铁橄榄石、磁铁矿、榍石、钛铁矿、金红石、磷灰石、十字石、独居石、锆石。对所含的重矿物进行归一化, 发现花土沟重矿物主要以闪石、黑云母、辉石、绿帘石为主(图 5)。14.4~14.1 Ma 黑云母含量最多, 其他时间段闪石最多。14.4~14.1 Ma 以绿帘石和辉石为主的基性和超基性重矿物含量为 33%, 与上下层区别较大。下油砂山组下部(20.0~14.4 Ma)含有 42% 绿帘石和辉石, 下油砂山组上部(14.1~12.4 Ma)含有 29% 绿帘石和辉石, 说明下油砂山组上、下部交界(14.4~14.1 Ma)期间物源可能发生了较大的变化, 上文的岩性描述也说明下油砂山组上下部岩性发生了较大的变化。上油

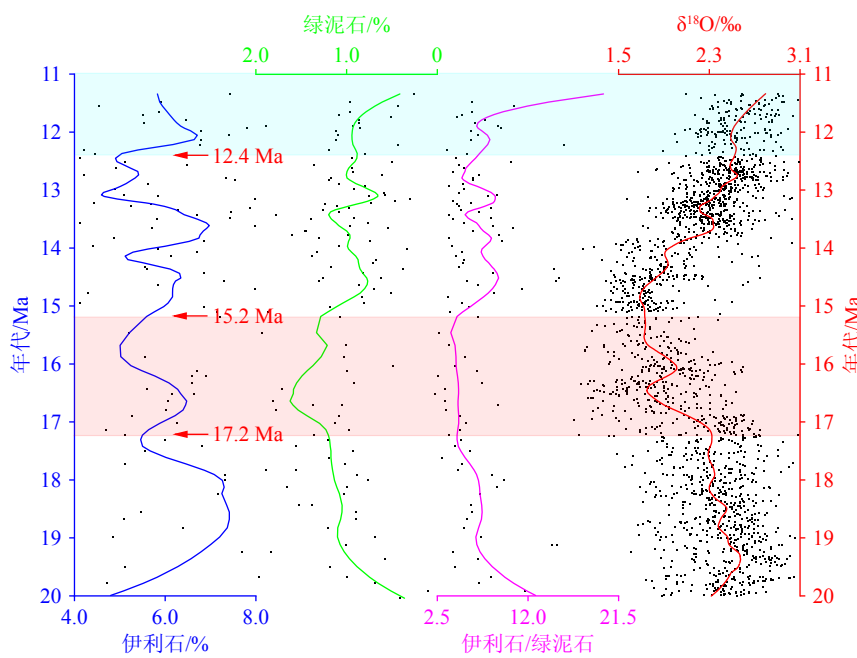


图4 花土沟剖面早—中中新世黏土矿物特征

实线为Origin窗口比例为0.2的Loess平滑曲线, $\delta^{18}\text{O}$ 引自文献[4]。

Fig.4 Early-middle Miocene clay mineral characteristics of Huatugou section

The color lines are the Loess smooth curves in window ratio of 0.2 with the Origin. The $\delta^{18}\text{O}$ data are cited from reference [4].

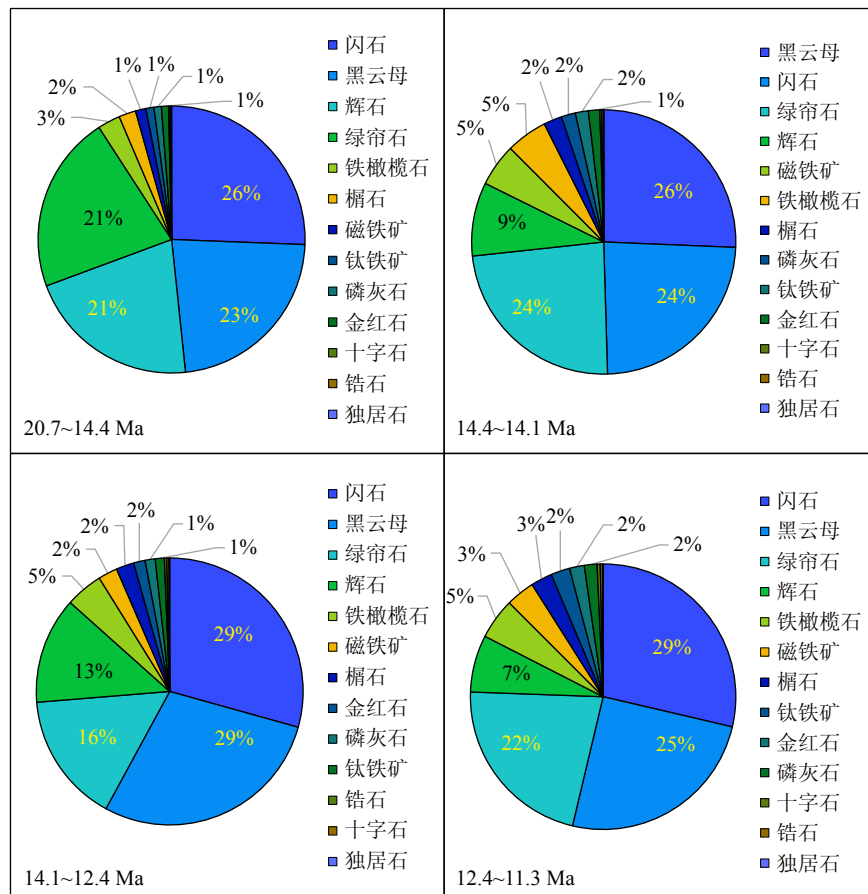


图5 花土沟剖面重矿物含量归一化饼图

Fig.5 Normalized pie chart of heavy mineral content in Huatugou section

砂山组含有 29% 的绿帘石和辉石, 与下油砂山组上部一致, 说明上油沙山组期间物源比较稳定。

4 讨论

4.1 柴达木盆地中新世构造运动与区域和全球气候的关系

提取 AMICS 统计的矿物颗粒为粒径小于 $4 \mu\text{m}$ 的黏土矿物, 可以排除全岩矿物组分中碎屑母岩信息和沉积环境等沉积分选对风化指标的影响, 可以较为灵敏地反映古气候信息。重矿物分析显示 20~15 Ma 闪石含量最高, 物源相对比较稳定; 该层沉积物为下油砂山组, 岩性基本相同, 属于湖泊边缘相沉积, 物源未发生变化。通过柴达木盆地花土

沟剖面黏土矿物分析(图 6A)显示, 20.0~15.2 Ma 气候逐渐变湿, 尤其是 17.2~15.2 Ma 伊利石/绿泥石比值为最低值, 与中新世适宜期气候一致, 盆地处于较为温暖湿润的气候环境。全球大气 CO_2 浓度(图 6K)^[63] 和海洋 $\delta^{18}\text{O}$ (图 6L)^[4] 都记录了 MMCO。柴达木盆地西北部 KC1 钻孔孢粉研究发现, 在 18~14 Ma 期间, 喜热孢粉数量明显增多, 旱生孢粉分类群百分比较低(图 6J), 对应 MMCO 期间温暖湿润的气候^[25, 27]。柴达木盆地花土沟剖面岩石磁学分析显示在 17.4~14.5 Ma 期间气候温暖湿润(图 6B)^[23]。柴达木盆地大红沟剖面磁学指标指示在中新世变暖过程降水量也有增加^[26]。陇中盆地黏土矿物显示 16~14 Ma 气候温暖湿润, 对应 MMCO^[64]。陇中盆地孢粉数据显示, MMCO 期间的植被主要以阔叶落叶林和针落叶阔叶混交林组成, 对应温暖潮湿

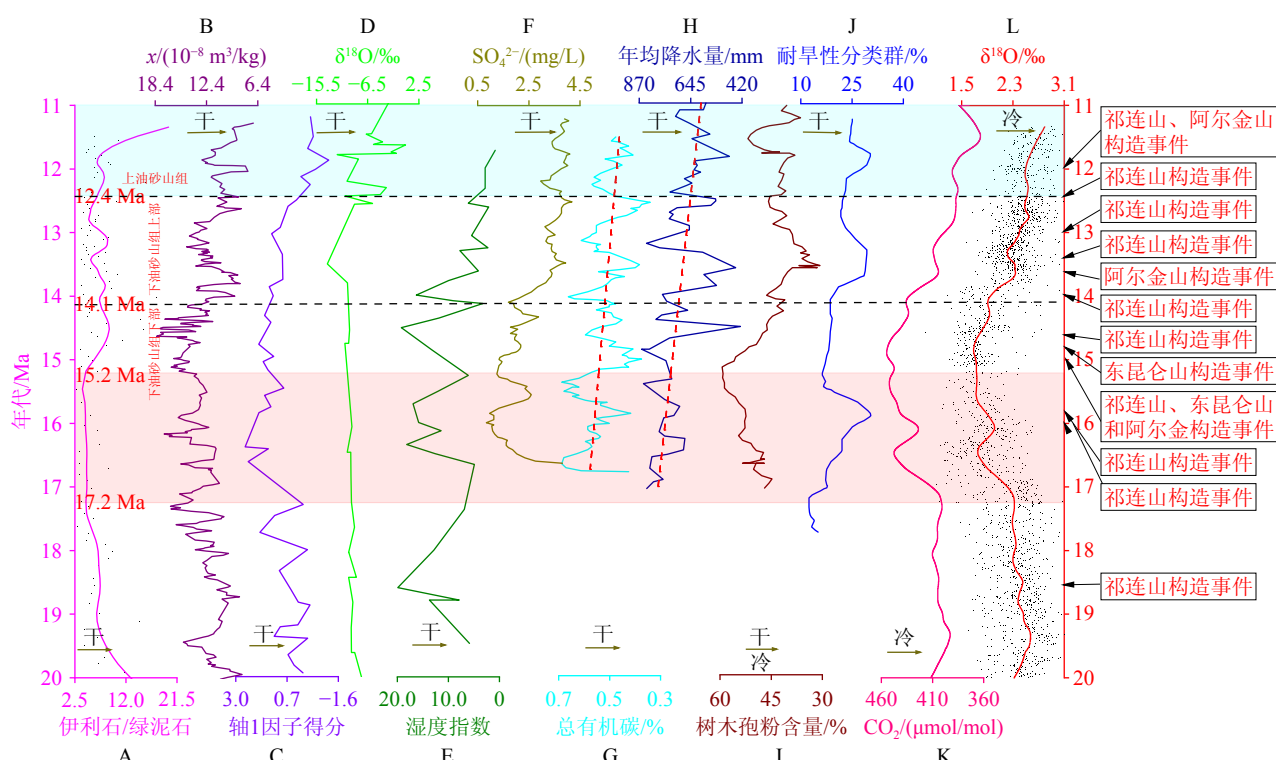


图 6 早—中中新世柴达木盆地与全球气候记录对比

A: 花土沟中新世伊利石/绿泥石(实线为 Origin 窗口比例为 0.2 的 Loess 平滑曲线), B: 花土沟剖面的磁化率(χ)^[23], C: 塔西河剖面主成分分析轴 1 因子得分的垂直变化^[6], D: 柴达木盆地西部 $\delta^{18}\text{O}(\text{‰}, \text{VPDB})$ ^[17], E: 寺口子剖面花粉记录的湿度指数^[68], F: 柴达木盆地红沟子剖面 SO_4^{2-} , G: 总有机碳记录^[24], H: 柴达木盆地年平均降水量^[69], I: 天水盆地燕湾剖面树木孢粉含量^[67], J: 柴达木盆地 KC1 岩芯花粉记录旱生分类群百分比^[25], K: 重建的全球大气 CO_2 浓度^[63], L: 全球海洋 $\delta^{18}\text{O}$ 记录^[4]。

Fig.6 Comparison in various proxies between the Early-Middle Miocene Qaidam Basin and global climatic records

A: Huatugou Miocene illite/chlorite (The solid line is the Loess smooth curve in the Origin window ratio of 0.2), B: magnetic susceptibility (χ) in Huatugou Section^[23], C: vertical variations in the factor scores of PCA axes 1 throughout the Taxihé section^[6], D: $\delta^{18}\text{O}(\text{‰}, \text{VPDB})$ in western Qaidam Basin^[17], E: humidity index from the pollen record of the Sikouzi section^[68], F: records of SO_4^{2-} , G: TOC from the Honggouzi section in the QB^[24], H: mean annual precipitation (ANPP) of the Qaidam Basin^[69], I: tree pollen percentages from the Yanwan section in Tianshui Basin^[67], J: percentages of the pollen of xerophytic taxa from core KC1 from the QB^[25], K: reconstructed global atmospheric CO_2 concentration^[63], L: global marine $\delta^{18}\text{O}$ record^[4].

的气候条件^[65]。西宁盆地岩性和岩石磁性显示 17~14 Ma 气候温暖湿润^[7]。天山北部的金沟河剖面孢粉记录指示 17.3~16.2 Ma 气候湿润^[66]。天山北部塔西河剖面孢粉学主成分分析显示 18~15 Ma 气候温暖潮湿, 对应中新世适宜期(图 6C)^[6]。天水盆地燕湾剖面树木孢粉显示, 在 17.1~14.7 Ma 植被主要由桦树、桦属和栎属的温带至暖温带森林为主, 表征气候温暖湿润(图 6 I)^[67]。这些证据均表明柴达木盆地 17.2~15.2 Ma 对应中新世暖期温暖湿润的气候(MMCO), 主要受全球变暖的影响。

15.2~14.4 Ma 伊利石/绿泥石比值增加, 变化趋势与全球气候类似, 可能受中新世气候转型期造成区域干旱化加强影响。15~14 Ma 期间全球海洋 $\delta^{18}\text{O}$ 开始增加(图 6L)^[4], 大气 CO_2 浓度开始减小(图 6K)^[63], 全球出现中中新世转型(MMCT)的降温事件。对中新世转型的记录前人已做了大量研究。柴达木盆地花土沟剖面岩石磁学分析显示, 在 14.5 Ma 以后气候变得干冷(图 6B)^[23]。柴达木盆地 SG-4 岩芯水生孢粉显示 14.4 Ma 气候变干, 主要受全球气候影响^[70]。柴达木盆地红沟子剖面地球化学数据显示, 在 17~11 Ma 期间 SO_4^{2-} 含量逐渐增加(图 6F), TOC 含量逐渐减少(图 6G), 主要受中新世气候转型影响, 14 Ma 柴达木盆地干旱化加剧^[24]。柴达木盆地年平均降水量显示 14 Ma 气候持续变干(图 6H)^[69]。天山北部的金沟河剖面孢粉记录显示 16.2 Ma 气候持续变干, 在 13.5 Ma 达到峰值^[66]。六盘山东侧寺口子剖面孢粉记录的湿度指标表明 14.25~11.34 Ma 湿度减弱(图 6E)^[68]。天水盆地燕湾剖面树木孢粉显示, 在 14.7~11.7 Ma 期间植被为森林或森林草原, 气候开始变干(图 6I)^[67]。

14.4~12.4 Ma 期间花土沟矿物指标变化与全球趋势气候不一致, 说明构造运动可能影响了该时段矿物组成。15 Ma 以后祁连山^[18, 28-34]、东昆仑山^[35-36]和阿尔金山^[19, 37-40]的构造事件明显增多, 柴达木盆地周边山体构造运动明显加剧。这些构造运动一方面影响了柴达木盆地的地形地貌, 使研究区的物源发生变化; 另一方面盆地周边的山体构造隆升也改变了区域大气环流模式, 增强的雨影效应改变了该区域气候特征, 使该时期区域气候与全球气候有所差别。图 6 所示的 14.1 Ma 和 12.4 Ma 分别是花土沟下油砂山组上下部界限和上下油砂山组界限, 这两个界限剖面岩性发生较大变化, 可能是期间的构造运动改变了沉积序列的矿物组成。上文中重矿物数据也指示 14.4~12.4 Ma 重矿物组成与之前显然不同, 尤其 14.4~14.1 Ma 发生了快速

的变化。14.4~12.4 Ma 的构造运动促使地层沉积物加入了新的物质, 扰乱了矿物组成指标得到的持续变干的气候序列趋势。柴达木盆地西部 $\delta^{18}\text{O}(\text{‰}, \text{VPDB})$ (图 6D)分析表明, 自 13 Ma 以来柴达木盆地的干旱可能与全球降温及青藏高原北部构造事件有关^[17]。以上证据说明 14.4~12.4 Ma 盆地可能受区域构造运动的影响。12.4~11.3 Ma 柴达木盆地区域气候与全球趋势一致, 持续干冷。柴达木盆地怀头他拉剖面化学风化指标指示 12.6 Ma 以来气候持续变干, 可能也指示了全球变冷的区域效应^[71]。

4.2 柴达木盆地中新世气候演化的驱动机制

新生代以来亚洲内陆气候变化的主控因素可能为全球变冷、山体和青藏高原隆升以及特提斯海退等^[12-16, 72-77]。主要的特提斯海退阶段大约发生在 34 Ma 之前^[15, 78]。本文研究的柴达木盆地样品时代属于 20 Ma 以后, 因此特提斯海退对柴达木盆地中新世的影响相对较小。柴达木盆地中新世气候主要受全球气候和构造事件的影响。20.0~14.4 Ma 伊利石/绿泥石比值变化趋势与全球海洋 $\delta^{18}\text{O}$ 记录^[4]和大气 CO_2 浓度^[63]变化一致, 说明该时段柴达木盆地主要受全球气候系统的影响。20.0~15.2 Ma 柴达木盆地逐渐变得温暖潮湿, 17.2~15.2 Ma 最为潮湿, 这是对中新世适宜期的响应。由于全球温度的升高会造成对流层水分增加及水平方向上水汽传输能力的提高^[79-80], 在其他降水条件不变的情况下, 能够引起区域降水量的增加, 这有利于绿泥石的保存, 而不利于伊利石的持续存在, 使伊利石/绿泥石值降低。15.2~14.4 Ma 伊利石/绿泥石比值增加, 受中新世气候转型期造成区域干旱化加强影响。全球变冷会使全球海面温度降低而减少蒸发量, 使到达陆地的水汽减少, 最终导致干旱化增强^[81-82]。同时, 全球变冷会使蒙古-西伯利亚高压增强, 引起冬季风增强, 造成其影响范围内干旱化增强^[76, 81, 83]。14.4~12.4 Ma 伊利石/绿泥石值波动降低, 与全球海洋 $\delta^{18}\text{O}$ 记录^[4]和大气 CO_2 浓度^[63]变化不一致。这可能与柴达木盆地西北部阿尔金、东昆仑山构造活动有关^[35-40], 这些构造事件改变了盆地沉积物矿物组成。12.4~11.3 Ma 伊利石/绿泥石比值升高, 与全球 $\delta^{18}\text{O}$ 变化一致, 可能与区域干旱化加强有关。因此, 伊利石/绿泥石比值在 20.0~14.4 Ma 和 12.4~11.3 Ma 主要受全球气候的控制, 而在 14.4~12.4 Ma 期间除了受全球气候的影响外, 可能还受到区域构造运动的改造。

显然, 柴达木盆地花土沟剖面中新世沉积物矿

物学研究显示, 区域气候主要受全球气候变化的影响, 物源区强烈构造运动也会对盆地沉积物矿物组成产生明显的改造。

5 结论

(1) 柴达木盆地 20.0~17.2 Ma 以来气候逐渐变得暖湿, 在 17.2~15.2 Ma 期间该区气候最为温暖湿润, 应该是中新世暖期区域响应, 受全球气候的影响。15.2~12.4 Ma 柴达木盆地受区域构造与中新世降温事件的共同影响, 盆地气候开始波动变干, 12.4~11.3 Ma 柴达木盆地持续变干。

(2) 重矿物物源分析表明, 14.4~12.4 Ma 柴达木盆地存在构造运动, 尤其 14.4~14.1 Ma 构造运动比较剧烈, 这些构造事件改变了盆地沉积物矿物组成。

致谢: 感谢中国科学院地球环境研究所李乐意、杨茂洁、沈俊杰、常小红、龙雪颖、易庭楠以及罗家馨的帮助。

参考文献 (References)

- [1] Kürschner W M, Kvaček Z, Dilcher D L. The impact of Miocene atmospheric carbon dioxide fluctuations on climate and the evolution of terrestrial ecosystems[J]. *Proceedings of the National Academy of Sciences of the United States of America*, 2008, 105(2): 449-453.
- [2] Greenop R, Foster G L, Wilson P A, et al. Middle Miocene climate instability associated with high-amplitude CO₂ variability[J]. *Paleoceanography*, 2014, 29(9): 845-853.
- [3] Flower B P, Kennett J P. The middle Miocene climatic transition: east Antarctic ice sheet development, deep ocean circulation and global carbon cycling[J]. *Palaeogeography, Palaeoclimatology, Palaeoecology*, 1994, 108(3-4): 537-555.
- [4] Zachos J, Pagani M, Sloan L, et al. Trends, rhythms, and aberrations in global climate 65 Ma to present[J]. *Science*, 2001, 292(5517): 686-693.
- [5] Böhme M. The Miocene Climatic Optimum: evidence from ectothermic vertebrates of Central Europe[J]. *Palaeogeography, Palaeoclimatology, Palaeoecology*, 2003, 195(3-4): 389-401.
- [6] Sun J M, Zhang Z Q. Palynological evidence for the Mid-Miocene Climatic Optimum recorded in Cenozoic sediments of the Tian Shan Range, northwestern China[J]. *Global and Planetary Change*, 2008, 64(1-2): 53-68.
- [7] Zan J B, Fang X M, Yan M D, et al. Lithologic and rock magnetic evidence for the Mid-Miocene Climatic Optimum recorded in the sedimentary archive of the Xining Basin, NE Tibetan Plateau[J]. *Palaeogeography, Palaeoclimatology, Palaeoecology*, 2015, 431: 6-14.
- [8] Hahn D G, Manabe S. The role of mountains in the South Asian monsoon circulation[J]. *Journal of the Atmospheric Sciences*, 1975, 32(8): 1515-1541.
- [9] 任雪萍. 柴达木盆地晚新生代古气候和化学风化研究 [D]. 兰州大学博士学位论文, 2021. [REN Xueping. Late Cenozoic paleoclimate and silicate chemical weathering research in the Qaidam Basin[D]. Doctor Dissertation of Lanzhou University, 2021.]
- [10] Tang H, Micheels A, Eronen J T, et al. Asynchronous responses of East Asian and Indian summer monsoons to mountain uplift shown by regional climate modelling experiments[J]. *Climate Dynamics*, 2013, 40(5-6): 1531-1549.
- [11] Raymo M E, Ruddiman W F. Tectonic forcing of late Cenozoic climate[J]. *Nature*, 1992, 359(6391): 117-122.
- [12] An Z S, Kutzbach J E, Prell W L, et al. Evolution of Asian monsoons and phased uplift of the Himalaya-Tibetan plateau since Late Miocene times[J]. *Nature*, 2001, 411(6833): 62-66.
- [13] Miao Y F, Herrmann M, Wu F L, et al. What controlled Mid-Late Miocene long-term aridification in Central Asia? —Global cooling or Tibetan Plateau uplift: a review[J]. *Earth-Science Reviews*, 2012, 112(3-4): 155-172.
- [14] 方亚会, 方小敏, 昝金波, 等. 西宁盆地总有机碳同位素记录的~39Ma 亚洲内陆急剧干旱事件 [J]. 地球环境学报, 2019, 10(5): 453-464. [FANG Yahui, FANG Xiaomin, ZAN Jinbo, et al. An Asian inland aridification enhancement event at ~39 Ma recorded by total organic carbon isotopes from Xining Basin[J]. Journal of Earth Environment, 2019, 10(5): 453-464.]
- [15] Bougeois L, Dupont-Nivet G, de Rafélis M, et al. Asian monsoons and aridification response to Paleogene sea retreat and Neogene westerly shielding indicated by seasonality in Paratethys oysters[J]. *Earth and Planetary Science Letters*, 2018, 485: 99-110.
- [16] Dupont-Nivet G, Krijgsman W, Langereis C G, et al. Tibetan plateau aridification linked to global cooling at the Eocene-Oligocene transition[J]. *Nature*, 2007, 445(7128): 635-638.
- [17] Li S E, Liu P X, Guan P, et al. Eocene to Miocene paleoclimate reconstruction of the northern Tibetan Plateau: constraints from mineralogy, carbon and oxygen isotopes of lacustrine carbonates in the western Qaidam Basin[J]. *Frontiers in Earth Science*, 2023, 11: 1217304.
- [18] Fang X M, Zhang W L, Meng Q Q, et al. High-resolution magnetostratigraphy of the Neogene Huaitoutala section in the eastern Qaidam Basin on the NE Tibetan Plateau, Qinghai Province, China and its implication on tectonic uplift of the NE Tibetan Plateau[J]. *Earth and Planetary Science Letters*, 2007, 258(1-2): 293-306.
- [19] Lu H J, Xiong S F. Magnetostratigraphy of the Dahonggou section, northern Qaidam Basin and its bearing on Cenozoic tectonic evolution of the Qilian Shan and Altyn Tagh Fault[J]. *Earth and Planetary Science Letters*, 2009, 288(3-4): 539-550.
- [20] Dong J B, Liu Z H, An Z S, et al. Mid-Miocene C₄ expansion on the Chinese Loess Plateau under an enhanced Asian summer monsoon[J]. *Journal of Asian Earth Sciences*, 2018, 158: 153-159.
- [21] Lebreton-Anberrée J, Li S H, Li S F, et al. Lake geochemistry reveals marked environmental change in Southwest China during the Mid Miocene Climatic Optimum[J]. *Science Bulletin*, 2016, 61(11): 897-910.

- [22] Miao Y F, Fang X M, Liu Y S, et al. Late Cenozoic pollen concentration in the western Qaidam Basin, northern Tibetan Plateau, and its significance for paleoclimate and tectonics[J]. *Review of Palaeobotany and Palynology*, 2016, 231: 14-22.
- [23] Guan C, Chang H, Yan M D, et al. Rock magnetic constraints for the Mid-Miocene Climatic Optimum from a high-resolution sedimentary sequence of the northwestern Qaidam Basin, NE Tibetan Plateau[J]. *Palaeogeography, Palaeoclimatology, Palaeoecology*, 2019, 532: 109263.
- [24] Song C H, Hu S H, Han W X, et al. Middle Miocene to earliest Pliocene sedimentological and geochemical records of climate change in the western Qaidam Basin on the NE Tibetan Plateau[J]. *Palaeogeography, Palaeoclimatology, Palaeoecology*, 2014, 395: 67-76.
- [25] Miao Y F, Fang X M, Herrmann M, et al. Miocene pollen record of KC-1 core in the Qaidam Basin, NE Tibetan Plateau and implications for evolution of the East Asian monsoon[J]. *Palaeogeography, Palaeoclimatology, Palaeoecology*, 2011, 299(1-2): 30-38.
- [26] Nie J S, Ren X P, Saylor J E, et al. Magnetic polarity stratigraphy, provenance, and paleoclimate analysis of Cenozoic strata in the Qaidam Basin, NE Tibetan Plateau[J]. *GSA Bulletin*, 2020, 132(1-2): 310-320.
- [27] Miao Y F, Fang X M, Wu F L, et al. Late Cenozoic continuous aridification in the western Qaidam Basin: evidence from sporopollen records[J]. *Climate of the Past*, 2013, 9(4): 1863-1877.
- [28] He P J, Song C H, Wang Y D, et al. Cenozoic deformation history of the Qilian Shan (northeastern Tibetan Plateau) constrained by detrital apatite fission-track thermochronology in the northeastern Qaidam Basin[J]. *Tectonophysics*, 2018, 749: 1-11.
- [29] Wang W T, Zheng W J, Zhang P Z, et al. Expansion of the Tibetan Plateau during the Neogene[J]. *Nature Communications*, 2017, 8: 15887.
- [30] Zhuang G S, Zhang Y G, Hourigan J, et al. Microbial and geochronologic constraints on the neogene paleotopography of northern Tibetan plateau[J]. *Geophysical Research Letters*, 2019, 46(3): 1312-1319.
- [31] Lease R O, Burbank D W, Clark M K, et al. Middle Miocene reorganization of deformation along the northeastern Tibetan Plateau[J]. *Geology*, 2011, 39(4): 359-362.
- [32] Wang W T, Zhang P Z, Pang J Z, et al. The Cenozoic growth of the Qilian Shan in the northeastern Tibetan Plateau: a sedimentary archive from the Jiuxi Basin[J]. *Journal of Geophysical Research: Solid Earth*, 2016, 121(4): 2235-2257.
- [33] Lin X, Zheng D W, Sun J M, et al. Detrital apatite fission track evidence for provenance change in the Subei Basin and implications for the tectonic uplift of the Danghe Nan Shan (NW China) since the mid-Miocene[J]. *Journal of Asian Earth Sciences*, 2015, 111: 302-311.
- [34] Wang W T, Zheng D W, Li C P, et al. Cenozoic exhumation of the Qilian Shan in the northeastern Tibetan Plateau: evidence from low-temperature thermochronology[J]. *Tectonics*, 2020, 39(4): e2019TC005705.
- [35] Mao L G, Xiao A C, Wu L, et al. Cenozoic tectonic and sedimentary evolution of southern Qaidam Basin, NE Tibetan Plateau and its implication for the rejuvenation of Eastern Kunlun Mountains[J]. *Science China Earth Sciences*, 2014, 57(11): 2726-2739.
- [36] Jolivet M, Brunel M, Seward D, et al. Neogene extension and volcanism in the Kunlun Fault Zone, northern Tibet: New constraints on the age of the Kunlun Fault[J]. *Tectonics*, 2003, 22(5): 1052.
- [37] Sun J M, Zhu R X, An Z S. Tectonic uplift in the northern Tibetan Plateau since 13.7 Ma ago inferred from molasse deposits along the Altyn Tagh Fault[J]. *Earth and Planetary Science Letters*, 2005, 235(3-4): 641-653.
- [38] Wu L, Xiao A C, Yang S F, et al. Two-stage evolution of the Altyn Tagh Fault during the Cenozoic: new insight from provenance analysis of a geological section in NW Qaidam Basin, NW China[J]. *Terra Nova*, 2012, 24(5): 387-395.
- [39] Ritts B D, Yue Y J, Graham S A, et al. From sea level to high elevation in 15 million years: Uplift history of the northern Tibetan Plateau margin in the Altun Shan[J]. *American Journal of Science*, 2008, 308(5): 657-678.
- [40] Chang H, Li L Y, Qiang X K, et al. Magnetostratigraphy of Cenozoic deposits in the western Qaidam Basin and its implication for the surface uplift of the northeastern margin of the Tibetan Plateau[J]. *Earth and Planetary Science Letters*, 2015, 430: 271-283.
- [41] 陈涛, 王欢, 张祖青, 等. 粘土矿物对古气候指示作用浅析 [J]. *岩石矿物学杂志*, 2003, 22(4): 416-420. [CHEN Tao, WANG Huan, ZHANG Zuqing, et al. Clay minerals as indicators of paleoclimate[J]. *Acta Petrologica et Mineralogica*, 2003, 22(4): 416-420.]
- [42] 汤艳杰, 贾建业, 谢先德. 粘土矿物的环境意义 [J]. *地学前缘*, 2002, 9(2): 337-344. [TANG Yanjie, JIA Jianye, XIE Xiande. Environment significance of clay minerals[J]. *Earth Science Frontiers*, 2002, 9(2): 337-344.]
- [43] 脱世博. 柴达木盆地东北部中新世沉积物粘土矿物变化特征与化学风化及其古气候意义 [D]. 兰州大学硕士学位论文, 2013. [TUO Shibo. Characteristic changes of the clay minerals, chemical weathering and paleoclimatic significance in the Miocene, Northeastern of the Qaidam Basin[D]. Master Dissertation of Lanzhou University, 2013.]
- [44] Winkler A, Wolf-Welling T, Stattegger K, et al. Clay mineral sedimentation in high northern latitude deep-sea basins since the Middle Miocene (ODP Leg 151, NAAG)[J]. *International Journal of Earth Sciences*, 2002, 91(1): 133-148.
- [45] Cheng F, Jolivet M, Fu S T, et al. Northward growth of the Qimen Tagh Range: a new model accounting for the Late Neogene strike-slip deformation of the SW Qaidam Basin[J]. *Tectonophysics*, 2014, 632: 32-47.
- [46] Yin A, Dang Y Q, Zhang M, et al. Cenozoic tectonic evolution of the Qaidam basin and its surrounding regions (Part 3): structural geology, sedimentation, and regional tectonic reconstruction[J]. *GSA Bulletin*, 2008, 120(7-8): 847-876.
- [47] Yin A, Dang Y Q, Zhang M, et al. Cenozoic tectonic evolution of Qaidam basin and its surrounding regions (part 2): wedge tectonics in southern Qaidam basin and the Eastern Kunlun Range[M]//Sears J W, Harms T A, Evenchick C A. Whence the Mountains? Inquiries into the Evolution of Orogenic Systems: A Volume in Honor of Raymond A. Price. Boulder: Geological Society of America, 2007: 369-390.
- [48] Meyer B, Tapponnier P, Bourjot L, et al. Crustal thickening in Gansu-

- Qinghai, lithospheric mantle subduction, and oblique, strike-slip controlled growth of the Tibet plateau[J]. *Geophysical Journal International*, 1998, 135(1): 1-47.
- [49] 孟庆泉. 柴达木盆地北缘晚新生代精细磁性地层学与沉积对构造的响应 [D]. 兰州大学博士学位论文, 2008. [MENG Qingquan. High resolution magnetostratigraphy in the north of Qaidam basin and the sedimentary response to tectonic since late cenozoic[D]. Doctor Dissertation of Lanzhou University, 2008.]
- [50] Métivier F, Gaudemer Y, Tapponnier P, et al. Northeastward growth of the Tibet plateau deduced from balanced reconstruction of two depositional areas: The Qaidam and Hexi Corridor basins, China[J]. *Tectonics*, 1998, 17(6): 823-842.
- [51] Wang E C E, Xu F Y, Zhou J X, et al. Eastward migration of the Qaidam basin and its implications for Cenozoic evolution of the Altyn Tagh fault and associated river systems[J]. *GSA Bulletin*, 2006, 118(3-4): 349-365.
- [52] Rieser A B, Neubauer F, Liu Y J, et al. Sandstone provenance of northwestern sectors of the intracontinental Cenozoic Qaidam basin, western China: tectonic vs. climatic control[J]. *Sedimentary Geology*, 2005, 177(1-2): 1-18.
- [53] Bush M A, Saylor J E, Horton B K, et al. Growth of the Qaidam Basin during Cenozoic exhumation in the northern Tibetan Plateau: inferences from depositional patterns and multiproxy detrital provenance signatures[J]. *Lithosphere*, 2016, 8(1): 58-82.
- [54] Xia W C, Zhang N, Yuan X P, et al. Cenozoic Qaidam basin, China: a stronger tectonic inverted, extensional rifted basin[J]. *AAPG Bulletin*, 2001, 85(4): 715-736.
- [55] Nesbitt H W, Young G M. Early Proterozoic climates and plate motions inferred from major element chemistry of lutites[J]. *Nature*, 1982, 299(5885): 715-717.
- [56] Gingele F X, De Deckker P, Hillenbrand C D. Late Quaternary fluctuations of the Leeuwin Current and palaeoclimates on the adjacent land masses: clay mineral evidence[J]. *Australian Journal of Earth Sciences*, 2001, 48(6): 867-874.
- [57] Bain D C. The weathering of chloritic minerals in some scottish soils[J]. *European Journal of Soil Science*, 1977, 28(1): 144-164.
- [58] Yemane K, Kahr G, Kelts K. Imprints of post-glacial climates and palaeogeography in the detrital clay mineral assemblages of an Upper Permian fluviolacustrine Gondwana deposit from northern Malawi[J]. *Palaeogeography, Palaeoclimatology, Palaeoecology*, 1996, 125(1-4): 27-49.
- [59] Ye C C, Yang Y B, Fang X M, et al. Evolution of Paleogene weathering intensity in the Qaidam Basin, northeastern Tibetan Plateau: insights from clay geochemistry[J]. *CATENA*, 2022, 213: 106162.
- [60] Rieu R, Allen P A, Plotze M, et al. Climatic cycles during a Neo-proterozoic "snowball" glacial epoch[J]. *Geology*, 2007, 35(4): 299-302.
- [61] Wang Z, Nie J S, Wang J P, et al. Testing contrasting models of the formation of the upper Yellow River using heavy-mineral data from the Yinchuan basin drill cores[J]. *Geophysical Research Letters*, 2019, 46(17-18): 10338-10345.
- [62] 和钟铧, 刘招君, 郭巍. 柴达木盆地北缘大煤沟剖面重矿物分析及其地质意义 [J]. *世界地质*, 2001, 20(3): 279-284, 312. [HE Zhonghua, LIU Zhaojun, GUO Wei. The heavy mineral analysis and its geological significance of Dameigou section in northern Qaidam basin[J]. *World Geology*, 2001, 20(3): 279-284, 312.]
- [63] van de Wal R S W, de Boer B, Lourens L J, et al. Reconstruction of a continuous high-resolution CO₂ record over the past 20 million years[J]. *Climate of the Past*, 2011, 7(4): 1459-1469.
- [64] Song Y G, Wang Q S, An Z S, et al. Mid-Miocene climatic optimum: clay mineral evidence from the red clay succession, Longzhong Basin, Northern China[J]. *Palaeogeography, Palaeoclimatology, Palaeoecology*, 2018, 512: 46-55.
- [65] Hui Z C, Zhang J, Ma Z H, et al. Global warming and rainfall: lessons from an analysis of Mid-Miocene climate data[J]. *Palaeogeography, Palaeoclimatology, Palaeoecology*, 2018, 512: 106-117.
- [66] Tang Z H, Ding Z L, White P D, et al. Late Cenozoic central Asian drying inferred from a palynological record from the northern Tian Shan[J]. *Earth and Planetary Science Letters*, 2011, 302(3-4): 439-447.
- [67] Hui Z C, Li J J, Xu Q H, et al. Miocene vegetation and climatic changes reconstructed from a sporopollen record of the Tianshui Basin, NE Tibetan Plateau[J]. *Palaeogeography, Palaeoclimatology, Palaeoecology*, 2011, 308(3-4): 373-382.
- [68] Jiang H C, Ding Z L. A 20 Ma pollen record of East-Asian summer monsoon evolution from Guyuan, Ningxia, China[J]. *Palaeogeography, Palaeoclimatology, Palaeoecology*, 2008, 265(1-2): 30-38.
- [69] Jia Y X, Wu H B, Zhang W C, et al. Quantitative Cenozoic climatic reconstruction and its implications for aridification of the northeastern Tibetan Plateau[J]. *Palaeogeography, Palaeoclimatology, Palaeoecology*, 2021, 567: 110244.
- [70] Wang H T, Wu F L, Yang L Y, et al. Miocene lake evolution in the western Qaidam Basin, northern Tibetan Plateau: evidence from aquatic-plant pollen[J]. *Journal of Asian Earth Sciences*, 2023, 250: 105634.
- [71] Bao J, Song C H, Yang Y B, et al. Reduced chemical weathering intensity in the Qaidam Basin (NE Tibetan Plateau) during the Late Cenozoic[J]. *Journal of Asian Earth Sciences*, 2019, 170: 155-165.
- [72] Zhang Z S, Wang H J, Guo Z T, et al. What triggers the transition of palaeoenvironmental patterns in China, the Tibetan Plateau uplift or the Paratethys Sea retreat?[J]. *Palaeogeography, Palaeoclimatology, Palaeoecology*, 2007, 245(3-4): 317-331.
- [73] Page M, Licht A, Dupont-Nivet G, et al. Synchronous cooling and decline in monsoonal rainfall in northeastern Tibet during the fall into the Oligocene icehouse[J]. *Geology*, 2019, 47(3): 203-206.
- [74] Wang X, Carrapa B, Sun Y C, et al. The role of the westerlies and orography in Asian hydroclimate since the late Oligocene[J]. *Geology*, 2020, 48(7): 728-732.
- [75] Ruddiman W F, Kutzbach J E. Forcing of late Cenozoic northern hemisphere climate by plateau uplift in southern Asia and the American west[J]. *Journal of Geophysical Research: Atmospheres*, 1989,

- 94(D15): 18409-18427.
- [77] Kutzbach J E, Prell W L, Ruddiman W F. Sensitivity of Eurasian climate to surface uplift of the Tibetan Plateau[J]. *The Journal of Geology*, 1993, 101(2): 177-190.
- [78] Kaya M Y, Dupont-Nivet G, Proust J N, et al. Paleogene evolution and demise of the proto-Paratethys Sea in Central Asia (Tarim and Tajik basins): role of intensified tectonic activity at ca. 41 Ma[J]. *Basin Research*, 2019, 31(3): 461-486.
- [79] Soden B J, Jackson D L, Ramaswamy V, et al. The radiative signature of upper tropospheric moistening[J]. *Science*, 2005, 310(5749): 841-844.
- [80] Held I M, Soden B J. Robust responses of the hydrological cycle to global warming[J]. *Journal of Climate*, 2006, 19(21): 5686-5699.
- [81] Guo Z T, Peng S Z, Hao Q Z, et al. Late Miocene-Pliocene development of Asian aridification as recorded in the Red-Earth Formation in northern China[J]. *Global and Planetary Change*, 2004, 41(3-4): 135-145.
- [82] Singh G. History of Aridland vegetation and climate: a global perspective[J]. *Biological Reviews*, 1988, 63(2): 159-195.
- [83] Song Y G, Fang X M, Chen X L, et al. Rock magnetic record of late Neogene red clay sediments from the Chinese Loess Plateau and its implications for East Asian monsoon evolution[J]. *Palaeogeography, Palaeoclimatology, Palaeoecology*, 2018, 510: 109-123.